Strain Sensing Through a Passive Wireless Sensor Array

Xiaohua Yi[a], Chia-Hung Fang[a], James Cooper[b], Chunhee Cho[a], Rushi Vyas[b],
Yang Wang[a], Roberto T. Leon[a], Manos M. Tentzeris[b]

[a] School of Civil and Environmental Engineering, Georgia Institute of Technology,
Atlanta, GA 30332, USA
[b] School of Electrical and Computer Engineering, Georgia Institute of Technology,
Atlanta, GA 30332, USA

ABSTRACT

This paper presents the strain sensing capability of a wireless and batteryless smart-skin sensor array. The sensor design is based on a folded patch antenna. When the patch antenna is under strain/deformation, its resonance frequency varies accordingly. The frequency variation can be easily interrogated and recorded by a wireless reader based on a backscattering mechanism. The patch antenna utilizes an inexpensive off-the-shelf radiofrequency identification (RFID) chip for signal modulation and anti-collision, in order to avoid interference among multiple sensors. Since the RFID chip harvests electromagnetic energy from the interrogation signal emitted by the reader, the patch antenna itself does not require other (internal) power source and, thus, serves as a batteryless and wireless strain sensor. In this preliminary investigation, several prototype folded patch antennas have been designed and manufactured to form a wireless strain sensor array. Tensile testing results of the wireless strain sensor show strong correlation between interrogated resonance frequency and strain experienced by the sensor. Minimum interference is observed among multiple sensors in the same neighborhood, when interrogated individually by a reader.

INTRODUCTION

Fatigue-induced fracture/crack in steel bridges is among the most common concerns for inspectors and owners (ASCE 2009). Currently, the Federal Highway Administration (FHWA) mandates biennial bridge deck evaluation and assessment. The primarily visual inspection can only detect cracks on the surfaces of a bridge structure (AASHTO 2009). Small-size cracks hidden under paint may grow to critical and dangerous sizes before the next inspection cycle. Early detection of cracks for fracture-critical-members of steel bridges has long been a challenging issue in bridge monitoring. Some existing technologies, including metal foil strain gages, fiber optic sensors, or ultrasonic testing, may assist in crack monitoring. However, most sensing systems either are too expensive for very dense instrumentation, or involve human-operated equipment that is not convenient for in-situ continuous deployment. These limitations make the existing technologies not practical for large-scale/large-area deployment and continuous monitoring in the field.

Recently, new wireless strain sensing approaches exploiting radiofrequency (RF) techniques have been investigated. The basic sensing mechanism is that when a small piece of electromagnetic (EM) antenna (usually with 2D shape) or a resonant circuit is under strain/deformation, the EM resonance frequency can change correspondingly. As a result, by measuring the resonance frequency shift of such an RF device, the strain experienced by the device can be derived. For example, wireless strain sensors are developed using inductive coupling mechanism; the resonance frequency shift under tensile strain is shown to be approximately linear (Jia *et al.* 2006; Loh *et al.* 2008). In addition, a microstrip patch antenna for measuring strain and detecting cracks in metallic structures is developed, based on EM backscattering mechanism (Tata *et al.* 2009; Deshmukh and Huang 2010). Nevertheless, the interrogation distance of an inductively coupling system is typically limited to a few inches. For previous backscattering wireless strain sensors, specialized circuitries (such as light-switching) are required for signal modulation.

To address these difficulties, a radiofrequency identification (RFID)-based folded patch antenna is developed as a passive wireless strain sensor for metallic structures (Yi *et al.* 2011a). The system utilizes backscattering mechanism and adopts a low-cost off-the-shelf RFID chip to reduce the design and manufacturing cost. Particularly, the RFID-based technology allows the sensor to be passive, i.e. to operate without other power source such as batteries (Finkenzeller 2003). The antenna substrate thickness effects are further studied for this folded patch antenna (Yi *et al.* 2011b), which shows that the interrogation range can be improved by increasing the thickness of the substrate. The sensing resolution and measurement limit of this prototype wireless strain sensor are investigated through extensive tensile tests (Yi *et al.* 2011c). It is shown that the prototype sensor can detect small strain changes lower than 20 $\mu\varepsilon$, and can perform well at a large strain higher than 10,000 $\mu\varepsilon$.

In this research, the sensing performance of a wireless strain sensor array is investigated. The array contains multiple wireless strain sensors in a close proximity, which potentially may cause interference among sensors during wireless interrogation. An anti-collision RFID mechanism is implemented to reduce the interference, and the performance of the sensor array is validated by tensile tests. The rest of the paper is organized as follows. First, the strain sensing mechanism for the wireless sensor is introduced. The anti-collision implementation for interrogating an array of sensors is described. Experimental results are then presented, demonstrating the performance of a sensor array formed by three passive wireless strain sensors. Finally, a summary and discussion of this work are provided.

WIRELESS STRAIN SENSING MECHANISM AND SENSOR DESIGN

Fig. 1 shows the passive wireless strain sensing system, which consists of an RFID reader and an RFID tag. Functioning as a wireless strain sensor, the RFID tag includes an antenna and an integrated circuit (IC) chip. The operating mechanism of the system relies on the backscattering mechanism, which refers to the reflection of EM wave from an illuminated object back to a source. Compared with inductive
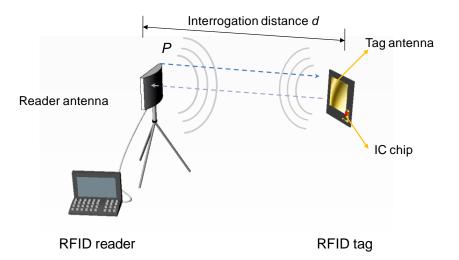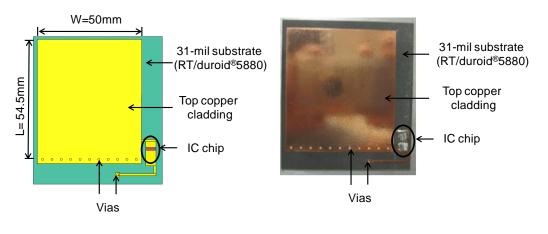
Fig. 1. Power transmission and backscattering in a passive RFID tag-reader system for wireless strain sensing

coupling, backscattering enables relatively large interrogation distance. The reader emits interrogation EM wave to the tag at power level *P*. If the power received by the tag is larger than the activation power threshold of the IC chip, the tag is activated and reflects EM wave back to the reader. Because the RFID tag receives all its operating power wirelessly from the reader, the operation is passive and no battery is needed for the tag.

An RFID-based folded patch antenna is designed as the passive wireless strain sensor (Yi *et al.* 2011a). Fig. 2 shows the design drawing and picture of a manufactured tag. The dimension for each part is shown in the figure too. The form

(a) Design drawing

(b) Manufactured wireless strain sensor

Fig. 2. RFID tag as wireless strain sensor

of patch antenna is adopted to provide good radiation performance on metallic objects. To further reduce the size of the patch antenna, vias through the substrate are used for connecting the top copper cladding with the ground plane on the back, forming a folded patch antenna. The adopted substrate material is Rogers RT/duroid®5880 with a thickness of 31 mils (0.79mm). The material is a glass microfiber reinforced poly-tetra-fluoro-ethylene (PTFE) composite with a dielectric constant ε_r of 2.20. The antenna resonance frequency at zero strain level, f_{R0}, can be estimated as:

$$f_{R0} = \frac{c}{4(L + L')\sqrt{\varepsilon_r}} \tag{1}$$

where c is the speed of light; L is the physical length of the top copper cladding; L' is the additional electrical length compensating fringing effect. When the antenna experiences strain deformation of ε in the longitudinal direction, the resonance frequency shifts to:

$$f_R = \frac{c}{4(1 + \varepsilon)(L + L')\sqrt{\varepsilon_r}} = \frac{f_{R0}}{1 + \varepsilon} \tag{2}$$

When strain ε is small, the resonance frequency changes approximately linearly with respect to strain:

$$f_R = f_{R0}(1 - \varepsilon + \varepsilon^2 - \varepsilon^3 + \cdots) \approx f_{R0}(1 - \varepsilon) \tag{3}$$

This approximately linear relationship indicates that by measuring the antenna resonance frequency, the applied strain can be derived.

MECHANISM OF THE SENSOR ARRAY INTERROGATION

Based on the dimension and material property of the prototype sensor, its resonance frequency at zero strain can be estimated according to Eq. (1):

$$f_{R0} = \frac{3 \times 10^8 \, \text{m/s}}{4 \times (54.5\text{mm} + 0.414\text{mm}) \times 10^{-3} \, \text{m/mm} \times \sqrt{2.2}} = 920.8 \, \text{MHz} \tag{4}$$

Here $L' = 0.414$mm is calculated according to the approximate equation for fringing effect (Balanis 1997). If two fabricated wireless strain sensors have the same dimension and material property, they also have the same initial resonance frequency at zero strain. Without an anti-collision mechanism available, multiple sensors in close proximity will respond to the interrogation signal from the reader simultaneously, interfering with each other. The IC chip integrated in the prototype wireless strain sensor provides a convenient solution to the interference problem, owing to its conformance to the Class-1 Generation-2 UHF RFID protocol (EPCglobal 2008). Under this protocol, the reader can issue a "SELECT" command to distinguish between multiple RFID tags in close proximity. The command requires a tag to respond to the reader only when selected by the reader, and the implementation details are described as follows.

The interrogation reader used in this work is the Tagformance Lite unit from Voyantic. The IC chip integrated in the prototype sensor is the SL3ICS1002 model from NXP Semiconductors (NXP Semiconductors 2011). The chip contains a 240-bit electronic product code (EPC) memory and a 64-bit tag identifier (TID). The 64-bit TID includes a 32-bit unique serial number, which potentially can be adopted for the tag identification. However, since the "SELECT" command implemented in the Tagformance Lite reader can only use the tag EPC code as an identifier, the EPC memory is utilized for the identification purpose. A LabVIEW program is implemented for enabling the Tagformance Lite reader to achieve the identification functionality. The program first writes a unique number to the EPC memory of each tag by the "WRITE" command in the Class-1 Generation-2 UHF RFID protocol. After the writing process, the tags are inventoried and ready for interrogation. Each sensor tag is sequentially selected by the LabVIEW program through the reader, according to the tag's unique EPC code among all sensors in proximity. Only the selected sensor actively responds and communicates with the reader, which avoids collision among multiple sensors.

The Tagformance Lite reader can sweep through an interrogation frequency range from 800 MHz to 1000 MHz, with a frequency resolution of 0.1 MHz. At each interrogation frequency, the reader varies the interrogation power (highest interrogation power is about 28 dBm) to determine the minimum threshold, i.e. least amount of interrogation power required to activate the IC chip. Once the IC chip is activated and selected, it modulates the stored identifier code and sends the code back to the reader through the tag antenna. The measurement resolution for the interrogation power threshold is 0.1 dBm. Through a USB 2.0 port, a computer interface is used to operate and retrieve measurement data from the reader.

As discussed in the previous section, the RFID tag antenna is designed with one specific resonance frequency. When the interrogation frequency f by the reader equals the resonance frequency of the tag, the best impedance matching is achieved between the tag antenna and the IC chip. In this scenario, the least amount of power needs to be transmitted by the reader for activating the IC chip. This means the interrogation power threshold plot $P(f)$ (measured by the reader) reaches minimum value at the resonance frequency, which is conceptually shown in Fig. 3. When there is no strain/deformation, the minimum power threshold occurs at resonance frequency f_{R0} (as discussed in Eq. (1)). When the antenna length changes due to strain ε in the
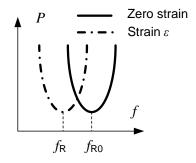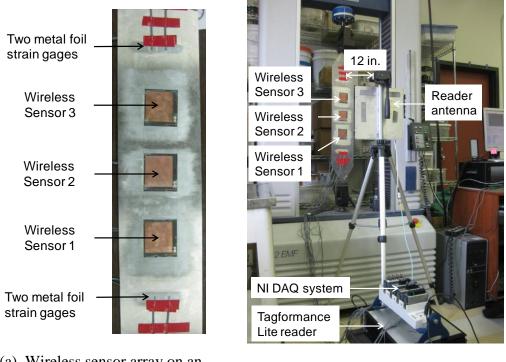

Fig. 3. Conceptual illustration of the resonance frequency shift due to strain

longitudinal direction, the resonance frequency changes to f_R (Eq. (2)). Accordingly, the $P(f)$ plot for the antenna under strain reaches minimum at f_R.

SENSOR ARRAY MEASUREMENT RESULTS

Tensile testing is conducted to study the strain sensing performances of a sensor array with three wireless sensors in close proximity. Fig. 4(a) shows the center area of the aluminum specimen, with three wireless strain sensors and four conventional strain gages (FLA-2-23-3LT, Texas Measurements, Inc) measuring the axial strain. Fig. 4(b) shows the experimental setup for the tensile testing with a 22-kip SATEC machine, similar to the setup for testing single wireless sensor. The reader antenna is mounted on a tripod, facing the middle sensor at a distance of 12 in. Through a coaxial cable, the reader antenna is connected with the Tagformance Lite reader unit. A National Instruments (NI) data acquisition system (DAQ) is adopted to collect strain data from four conventional metal foil strain gages.

The force applied by the testing machine is configured so that approximately a 50$\mu\epsilon$ increment is achieved at each loading step. The received power in dBm scale, $P(f)$, is measured by the Tagformance Lite reader at each loading step. To reduce the effect of measurement noise, a total of fifteen measurements are taken for each strain level and the average is calculated at every interrogation frequency f:

(a) Wireless sensor array on an aluminum specimen

(b) Experimental setup

Fig. 4. Experimental setup for the tensile test with a wireless sensor array

$$\overline{P}(f) = \frac{1}{15} \sum_{i=1}^{15} \left[P^i(f) \right] \tag{5}$$

where $\overline{P}$ is the average interrogation power threshold in dBm; $P^i(f)$ is the interrogation power threshold in dBm from the ith measurement. Fig. 5(a) shows the $\overline{P}(f)$ plot for Sensor 1 at different strain levels. The strain levels, shown in the legend of Fig. 5(a), are calculated as the average among four axial strain gages. As described in previous section, for each strain level, the interrogation power threshold reaches its minimum value at the resonance frequency. The interrogation power thresholds for the other two sensors are plotted Fig. 6(a) and Fig. 7(a), respectively.
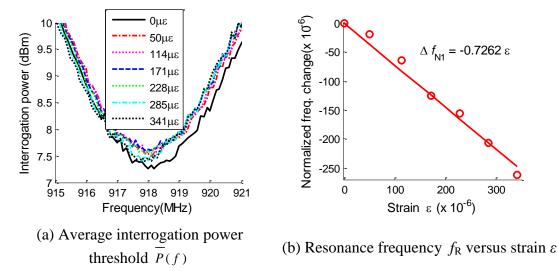

(a) Average interrogation power threshold $\overline{P}(f)$

(b) Resonance frequency f_R versus strain ε

Fig. 5. Tensile testing results for Sensor 1

(a) Average interrogation power threshold $\overline{P}(f)$

(b) Resonance frequency f_R versus strain ε

Fig. 6. Tensile testing results for Sensor 2

(a) Average interrogation power
threshold $\overline{P}(f)$

(b) Resonance frequency f_R versus strain ε
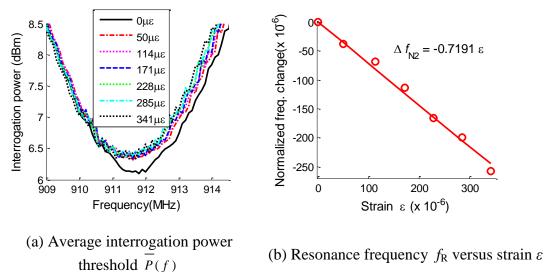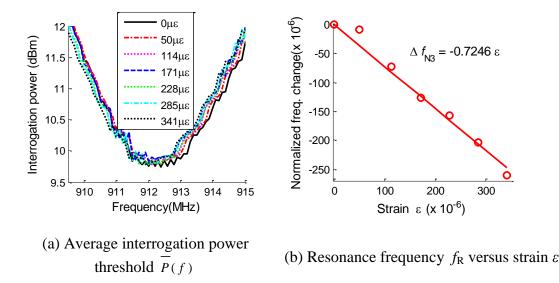
Fig. 7. Tensile testing results for Sensor 3

Since the valley area of the $\overline{P}(f)$ plot is relatively flat, the precise resonance frequency is not obvious from the plot at each strain level. To resolve this difficulty, a 4th order polynomial curve fitting is first performed to the valley area of each $\overline{P}(f)$ plot. The value of the fitted 4th order polynomial is re-calculated at a frequency step of 0.001 MHz, in order to identify the resonance frequency at every strain level.

Due to fabrication and installation tolerance, the initial resonance frequency of each wireless sensor at zero strain, f_{R0}, can be slightly different. For the three sensors tested in this work, the initial resonance frequency is identified as 918.127 MHz, 911.681 MHz, and 912.326 MHz, respectively. When the resonance frequency shifts to f_R due to strain ε, a normalized frequency change, Δf_N, can be calculated to offset the effect of different initial resonance frequencies:

$$\Delta f_N = \frac{f_R - f_{R0}}{f_{R0}} \qquad (6)$$

Since f_R reduces approximately linearly when strain ε increases (Eq. (3)), it can be shown that the normalized frequency change Δf_N is approximately proportional to strain:

$$\Delta f_N \approx s_N \varepsilon \qquad (7)$$

Here s_N represents the normalized strain sensitivity. Using the experimental data, normalized frequency changes are calculated and plotted against strain in Fig. 5(b), Fig. 6(b), and Fig. 7(b), for each wireless sensor. The normalized strain sensitivity s_N is shown to be -0.7262, -0.7191, and -0.7246, respectively. For example, $s_N = -0.7246$ means 1$\mu\varepsilon$ in the aluminum specimen causes the resonance frequency of the wireless sensor to reduce by 0.7246 ppm (parts per million), i.e. 0.00007246 %.

Although the results illustrate limited interference between neighboring sensors, certain interference still exists. This is inevitable due to the electromagnetic coupling between adjacent sensors. Even though only the selected RFID tag responds to the reader with modulated EM signals, other RFID tag antennas still reflect un-modulated EM waves to the reader. Because all three RFID tag antennas have very close resonance frequencies, the EM reflection still causes interference. Further study is needed to improve the consistency. For example, the interference can be reduced by designing wireless sensors with somewhat different initial resonance frequencies at zero strain level. Nevertheless, current level of performance can be adequate for a qualitative measurement of stress concentration.

CONCLUSION

This paper presents the strain sensing capability of a prototype wireless strain sensor array, whose design is based on a folded patch antenna. A LabVIEW interrogation program for the reader is implemented to avoid interference among neighboring sensors. The strain sensing performance of each sensor in the array is close to the performance previously reported for a single sensor. This means the interference between neighboring sensors does not significantly affect the overall performance of the sensor array. Although the current level of performance can be sufficient for a qualitative measurement of stress concentration, future studies are needed to improve the sensitivity consistency.

Since the resonance frequency of the wireless strain sensor is correlated with the antenna size, sensor footprint can be significantly reduced in future studies by increasing operating frequency. On the other hand, other antenna forms that can fold the electrical length, such as slotted antennas can also be exploited to reduce the antenna size. In addition, longer interrogation distance can be achieved by adopting a more directive antenna with higher gain.

ACKNOWLEDGEMENT

REFERENCES

AASHTO. (2009). *Manual of Bridge Evaluation*, American Association of State Highway & Transportation Officials, Washington D.C.

ASCE. (2009). *Report Card for America's Infrastructure*. American Society of Civil Engineers, Reston, VA.

Balanis, C. A. (1997). *Antenna Theory: Analysis and Design*. John Wiley & Sons, New York.

Deshmukh, S., and Huang, H. (2010). "Wireless interrogation of passive antenna sensors." *Measurement Science and Technology*, 21(3), 035201.

EPCglobal, I. (2008). *EPC^{TM} Radio-frequency Identity Protocols Class-1 Generation-2 UHF RFID Protocol for Communications at 860 MHz-960 MHz* Version 1.2.0, EPCglobal Inc.

Finkenzeller, K. (2003). *RFID Handbook*. John Wiley & Sons, New York.

Jia, Y., Sun, K., Agosto, F. J., and Quinones, M. T. (2006). "Design and characterization of a passive wireless strain sensor." *Measurement Science and Technology*, 17(11), 2869-2876.

Loh, K. J., Lynch, J. P., and Kotov, N. A. (2008). "Inductively coupled nanocomposite wireless strain and pH sensors." *Smart Structures and Systems*, 4(5), 531-548.

NXP Semiconductors. (2011). *Product Short Datasheet SL3ICS1002/1202*, NXP Semiconductors, Eindhoven, The Netherlands.

Tata, U., Huang, H., Carter, R. L., and Chiao, J. C. (2009). "Exploiting a patch antenna for strain measurements." *Measurement Science and Technology*, 20(1), 015201.

Yi, X., Wu, T., Wang, Y., Leon, R. T., Tentzeris, M. M., and Lantz, G. (2011a). "Passive wireless smart-skin sensor using RFID-based folded patch antennas." *International Journal of Smart and Nano Materials*, 2(1), 22-38.

Yi, X., Wu, T., Lantz, G., Wang, Y., Leon, R. T., and Tentzeris, M. M. (2011b)."Thickness variation study of RFID-based folded patch antennas for strain sensing." *Proceedings of SPIE, Sensors and Smart Structures Technologies for Civil, Mechanical and Aerospace Systems*, San Diego, CA, USA.

Yi, X., Wu, T., Lantz, G., Cooper, J., Cho, C., Wang, Y., Tentzeris, M. M., and Leon, R. T. (2011c)."Sensing resolution and measurement range of a passive wireless strain sensor." *Proceedings of the 8th International Workshop on Structural Health Monitoring*, Stanford, CA, USA.